Silicon Mechanical Sensors for High-Temperature Control Systems.
Design principles for monolithic IPT for a temperature range of 0–300 °C.

Michael Tikhomirov
1989

Abstract

This chapter outlines principles for designing monolithic integrated piezoresistor transducers (IPTs) in silicon mechanical sensors for automatic control systems operating in the 0–300°C temperature range. Experimental investigations focus on electrophysical, metrological, and operational characteristics to minimize geometrical parameters, temperature errors, and extend the upper operational limit.

For IPTs with isolating p-n junctions, constraints on minimum contact areas ($b_{min} = 30{\times}10^{-4}\ cm$) and channel widths are determined to limit normalized null output instability ($\gamma_{mc0} \leq 0.03$). Temperature dependencies of reverse current density reveal influences from perimeter-to-area ratio ($K_{p-n} = 500–700 cm^{-1}$) and corner count ($n_{p-n} \leq 8$), enabling upper limits of 250–300°C at $A_{p-n} < 2{\times}10^{-4}\ cm^2$. Diffusion and ion-implantation doping methods yield optimal resistivities ($\rho_{ch} = 2–8{\times}10^{-2}\ \Omega \cdot cm$) for auto-thermal compensation, with intrinsic errors ≤1–5%.

For distributed-parameter IPTs without p-n junctions, elastic elements regulate output temperature dependence, enhancing reliability above 200°C. Compensation conditions ($\Gamma_{mc}^{dp} = 0$) are derived, with experimental validation showing temperature ranges of -60 to 325°C for $\rho_{ee} = 0.5–10 \Omega \cdot cm$ and design parameter $H_{ee}/a \geq 0.3$.

Conclusions formulate error minimization principles, including thermal compensation schemes (accuracy <0.05%/°C) and tuning methods reducing systematic errors >10-fold, supporting compact, high-precision sensors in harsh environments.

From the results of the analysis in Chapter 1, the design problems arise for which additional studies of the electrophysical, metrological, and operational characteristics of IPT elements in the range of temperatures $(0 \div 300)^{\circ}C$ are necessary. The practical use of the results of the studies performed in Chapter 2 under certain conditions and assumptions also requires experimental refinements. Therefore, the purpose of this chapter is to experimentally investigate and determine the initial data required for the further design of specific IPT designs.

1. Designing an IPT with an Isolating P-N Junction

The minimization of the geometrical parameters of the topological structure MC in Fig.12 depends on the constraints on the minimum values of the contact areas b , length $(a-b)$ and width d_{ch} of the piezoresistive channels. The determination of minimum size constraints b_{min} is related to the experimental dependence of the temperature instability parameter γ_{mc0} of the normalized null output K_{mc0}, equal to

$$\gamma_{mc0} = \frac{K_{mc0}\left(T_{per}\right) - K_{mc0}\left(T_0\right)}{K_{mc0}\left(T_0\right) \cdot \left(T_{per} - T_0\right)} \cdot 100\%. \qquad (55)$$

from the change in the contact area "Al-Si" A_c, equal to $A_c = b_c^2$. At the known values of b_{min}, a further decrease in the geometric dimensions of MC (that is, the junction area of the insulation $p-n$) is associated with a decrease in the geometric parameters ($(a-b)$ and d_{ch} , which are related by the input resistance rating R_{in} and the surface resistance R_s of the layer PCH by relation.

$$\frac{R_{in}}{R_s} = \frac{a-b}{d_{ch}} \qquad (56)$$

The value of R_{in} is determined by the standard values $(95-1520)\ \Omega$ [1] [2]. According to [3], R_s for ion alloyed PCH is determined by the value $R_s^{ion} = 85\ \Omega/\square$ and for diffusive (if the value $x_j = 2.5 \cdot 10^{-4}\ cm$) $R_s^{dif} = (85 \div 320)\ \Omega/\square$. Decreasing the width of PCH, provided that $d_{ch} < b_{min}$, leads to an increase in the parameter $K_{p-n} = \frac{P_{p-n}}{A_{p-n}}$ (which is obvious from relations (37,38)) in relation (43). In this case, finding the upper bound of the operating temperature range for the real design IPT using the dependences in Fig.14 would be incorrect. The restrictions on the minimum values $d_{ch\,min}$ will be determined by experimental studies of the dependence of the temperature change of the inverse current density on the parameter K_{p-n}.

For the idealized structure of an isolating $p-n$ junction, it is assumed that the concentration of ionized atoms that determine the area of the volume charge and the related electric field strength are uniformly distributed in the direction of the y-axis coinciding with the metallurgical boundary of the transition. In real $p-n$ junctions at the corners of rectangular elements MC should increase the concentration of ionized atoms, which, apparently, will lead to changes in the parameters determining the generative surface and volume components of the reverse current, and thus to dependence of J_{rev} on the number n of these corners in the topological structure.

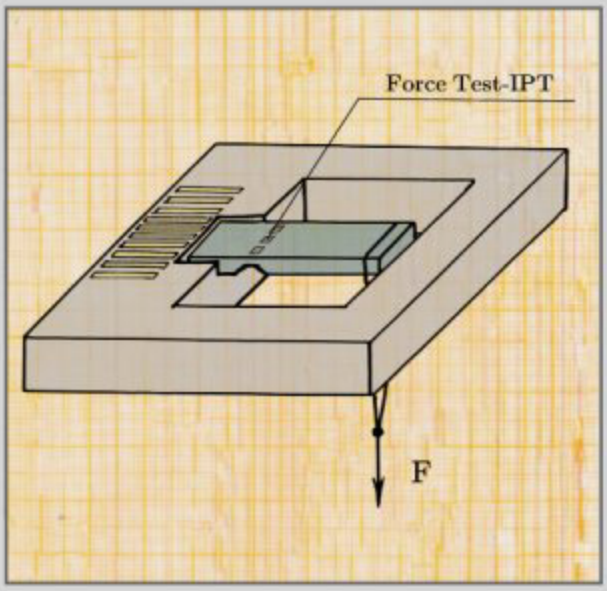

Figure 18. View of the beam force Test-IPT 5.E.2251.130.00.00.000.

The breakdown voltage of an idealized p-n junction of relation (44) was calculated without taking into account the influence of the surface on the electrical insulation strength, where adsorbed ions are always present, creating conditions for the development of avalanches earlier than in the volume [4]. From the results obtained in [5], V_{br} depends on the resistivity of EE, the type of transition, the environment and the surface condition. The real breakdown stresses for the experimental samples IPT were found to be $(5 \div 10)\ V$ and $(20 \div 50)\ V$ if the resistivity of the elastic element region is $0.5\ \Omega \cdot cm$ and $4.5\ \Omega \cdot cm$, respectively (PCH doping was done by boron ion implantation). It is likely that for most IPT with $\rho_{ee1} = 0.5\ \Omega \cdot cm$, where the breakdown voltages are proportional to the standard sensor supply voltages, the insulation properties will not be satisfactory. Therefore, single-crystal silicon of p-type orientation (001) with resistivity $\rho_{ee1} = 4.5\ \Omega \cdot cm$ was chosen to make experimental samples IPT.

The beam test-IPT forces 5E.2251.130.00.00.000 contain specially designed (according to the stated research objectives) test MC with different geometrical parameters. Fig.18 shows the general view of the force IPT, and the table (Fig.19) shows the investigated topological structures of MC and their geometrical parameters.

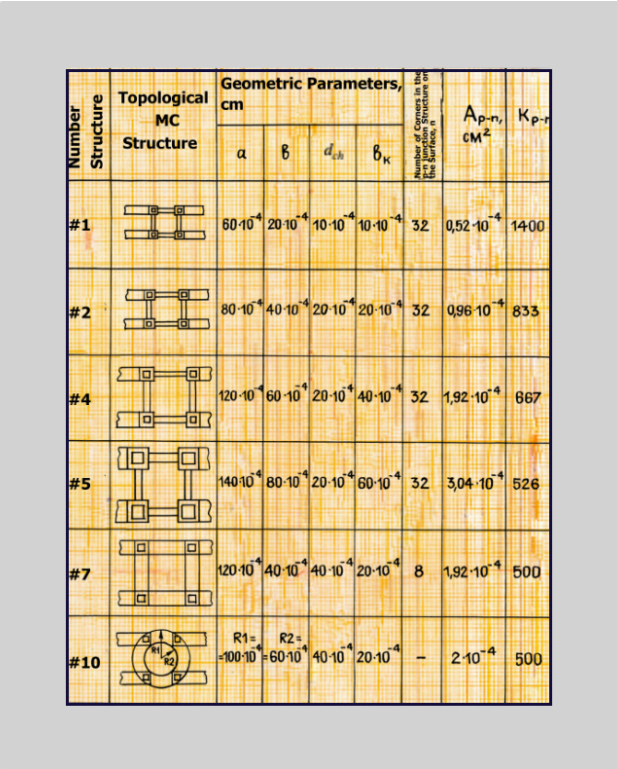

Number Structure	Topological MC Structure	Geometric Parameters, cm				Number of Corners in the p-n Junction Structure on the Surface, n	A_{p-n}, cm^2	K_{p-n}
		a	β	d_{ch}	β_K			
#1		$60\cdot10^{-4}$	$20\cdot10^{-4}$	$10\cdot10^{-4}$	$10\cdot10^{-4}$	32	$0{,}52\cdot10^{-4}$	1400
#2		$80\cdot10^{-4}$	$40\cdot10^{-4}$	$20\cdot10^{-4}$	$20\cdot10^{-4}$	32	$0{,}96\cdot10^{-4}$	833
#4		$120\cdot10^{-4}$	$60\cdot10^{-4}$	$20\cdot10^{-4}$	$40\cdot10^{-4}$	32	$1{,}92\cdot10^{-4}$	667
#5		$140\cdot10^{-4}$	$80\cdot10^{-4}$	$20\cdot10^{-4}$	$60\cdot10^{-4}$	32	$3{,}04\cdot10^{-4}$	526
#7		$120\cdot10^{-4}$	$40\cdot10^{-4}$	$40\cdot10^{-4}$	$20\cdot10^{-4}$	8	$1{,}92\cdot10^{-4}$	500
#10		R1 = $100\cdot10^{-4}$	R2 = $60\cdot10^{-4}$	$40\cdot10^{-4}$	$20\cdot10^{-4}$	–	$2\cdot10^{-4}$	500

Figure 19. Topological structures and geometrical parameters of MC on test-IPT force transducer

Two methods of PCH doping were implemented in the fabrication of the force test-IPT :

- boron ion implantation with a doping dose of $2 \cdot 10^{15}\ cm^{-2}$ and surface resistivity $R_{s\,ee} = 85\ \Omega/\square$;
- diffusion of boron with average resistivity values PCH (where we can expect in the range $(0 \div 300)^{\circ}C$ "auto-compensation" of temperature sensitivity changes when feeding MC with stabilized current) $0.02\ \Omega \cdot cm$, $0.03\ \Omega \cdot cm$ and $0.06\ \Omega \cdot cm$

For all IPT variants, diffusion low-resistance contact areas with surface resistivity formed $(10 \div 12)\ \Omega/\square$.

To evaluate the electrophysical characteristics of IPT with an insulating $p-n$ junction, the following parameters and computational relationships have been used:

- input resistance MC,
$$R_{in} = \frac{V_{in}}{I_{in}} \qquad (57)$$
- normalized null output MC,
$$K_{mc0} = \frac{V_{out\,0}}{V_{in}} \qquad (58)$$
- reverse current I_{rev} when the insulating $p-n$ junction is reverse biased by a $5\ V$ voltage;
- sensitivity coefficient of the PCH at the assumed equality $|K_{\parallel}| = |K_{\perp}|$, equal to
$$K_{ch} = \frac{V_{in\,F} - V_{out\,0}}{V_{in} \cdot \varepsilon_{x_0}} \qquad (59)$$
where $V_{in\,F}$ is the output of MC when the console of the elastic element is loaded with a load F; ε_{x_0} is the strain at the location of MC;
- intrinsic error for pressure sensors not more than $\pm 1\%$; for sensors of vibration acceleration (acceleration sensors) not more than $\pm 5\%$;
- approximation coefficients of temperature dependence of input resistance MC $R_{in} = R_{in\,0}\left[1 + A_1\,(T - T_0) + A_2(T - T_0)^2\right]$, A_1 and A_2 were determined by joint measurements [6] $R_{in\,1}$, $R_{in\,2}$,$R_{in\,0}$ at temperatures respectively $T_1 = 300\ K$, $T_2 = 500\ K$, $T_0 = 400\ K$;
- approximation coefficients of the temperature dependence of the gauge factor PCH (2.19) K_A, K_B, K_C were determined by joint measurements $K_{ch\,1}$, $K_{ch\,2}$, $K_{ch\,0}$ at temperatures

$T_1 = 300\ K,\ T_2 = 500\ K,\ T_0 = 400\ K$ respectively.

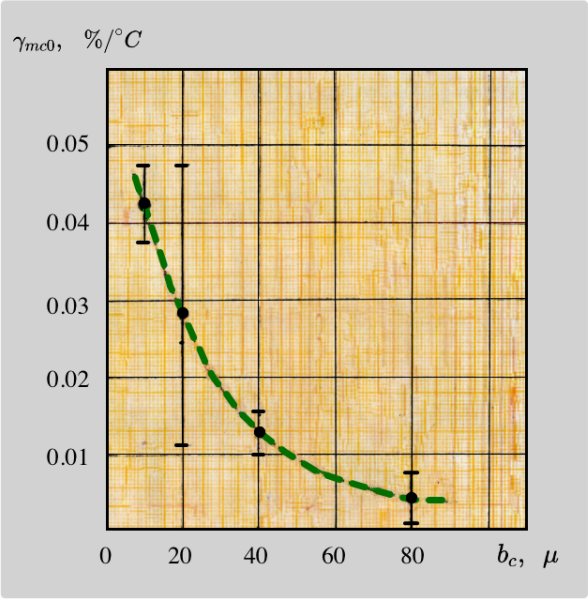

Figure 20. Dependence of the temperature instability parameter γ_{mc0} of the initial MC transfer coefficient on the contact size b_c .

Fig.20 shows the dependence of the temperature instability coefficient of K_{mco} on the value of b_c when feeding MC with stabilized voltage. For pressure sensors with intrinsic error $\pm 1\%$, according to [1:1], the limit value of the complementary temperature error should not be greater than $0.06\%/^\circ C$. When selecting the boundary value γ_{mc0}, it was taken into account that the experimentally obtained dependence in the graph of Fig.20 gives an estimate of the influence of contact resistances only. For this purpose, during the measurements IPT were not fixed in the case and had a thickness $EE\ H_{ee} \geqslant 100 \cdot 10^{-4}$ cm. As shown in [7] [8], at real values of $H_{ee} = (10 \div 100) \cdot 10^{-4}\ cm$ the temperature-dependent initial stress state of the transducer due to the difference in $\alpha_l^{ch} (= \alpha_l^{Si})\ \alpha_l^{SiO_2};\ \alpha_l^{il};\ \alpha_l^{ee} (= \alpha_l^{si});\ \alpha_l^{rb}$ increases γ_{mc0} by $(0.02 \div 0.03)\%/^\circ C$. The boundary value of γ_{mc0} is taken to be $(0.03)\%/^\circ C$. Then the minimum contact dimensions $b_{c\,min}$ (from the graph in Fig.20) and the diffusion contact region b_{min} at the 5-micrometer process gap between the contact and the $p-n$ junction are $b_{c\,min} = 20 \cdot 10^{-4}\ cm$, $b_{min} = 30 \cdot 10^{-4}\ cm$.

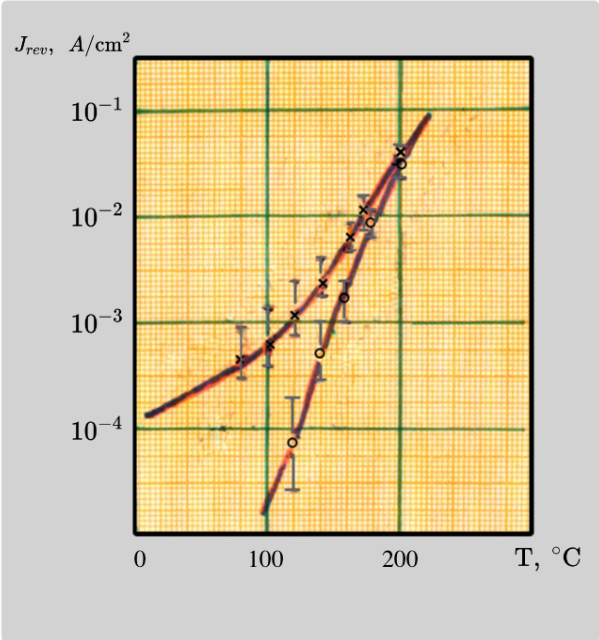

Figure 21. Dependence of insulating p-n junction reverse current density for MS #5:
✖ - with diffusion PCHs;
o - with ion-alloyed PCHs.

Fig.21 shows a graph of the temperature dependence of the reverse current density of insulating p-n junctions with ion alloy and diffusion PCH for the test structure $MC\#5$ with $A_{p-n} = 3 \cdot 10^{-4} cm^2$. The noticeable difference in the variation for the experimental samples at temperatures below +150 C can be explained by the influence of the variation on the surface recombination rate S_0. The temperature dependence of the diffusion component of the reverse current at temperatures above $+150^{\circ}C$ becomes determinative, and the dependences for the experimental samples approach each other.

The results of the investigation of the influence of the geometric parameters of the topological structure of MS K_{p-n} and n on the insulating properties of the $p-n$-junction are shown in Fig.22. Temperature dependences of the reverse current density of different test structures define three areas.

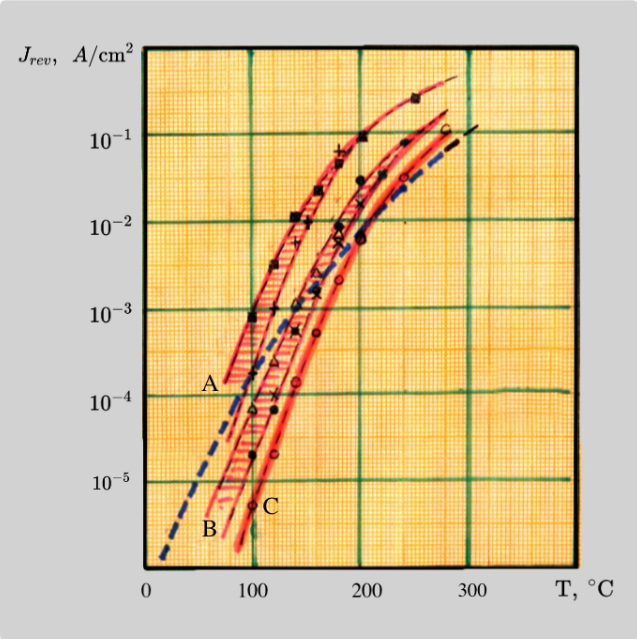

Figure 22. Temperature dependences of the reverse current density of p-n junction insulating ion-alloyed and diffusion contact areas MC: ----- calculated from (45)

■— #1; + — #2; △- #4; •- #5; ×— #7; o — #10

(A) The high-level region of reverse current density *"A"* is made up of dependencies for structures where the number n is maximal ($n = 32$), and K_{p-n} is in the range $800 - 1400(\#1, \#2)$. In this case, the extension of the upper bound of the operating temperature range to values $T_{per} \geqslant 200^{\circ}C$ is unlikely. The areas of the insulating $p-n$-junctions should be $A_{p-n} \leqslant 2 \cdot 10^{-5}\ cm^2$, that is, more than 3 times less than the limit value previously defined of the total area of the four contact sites MC.

(B) The J_{rev} *"B"* plot of mean values J_{rev} *"B"* belongs to the MC dependence of structures where the number of n angles is 32 and 8, but K_{p-n} is in the range $(500 \div 700) cm^{-1}$ ($\#4, \#5, \#7$). Here, a realistic design for high temperatures is MC #7 with parameters $K_{p-n} = 500\ cm^{-1}$ and $n = 8$ with $p-n$ transition area $A_{p-n} \leq 2 \cdot 10^{-4}\ cm^2$.

(C) The *"C"* cross section, for a MC #10 ring structure with $K_{p-n} = 500\ cm^{-1}$, at temperatures $T > 180^{\circ}C$, is in good agreement with the calculated $\boldsymbol{J}_{\text{rev}}\ (T)$ dependence. Differences at temperatures $T < 180^{\circ}C$ can be explained by the fact that the calculated dependence $\boldsymbol{J}_{\text{rev}}\ (T)$ selected a maximum limit value S_0 equal to $S_0 = 1 \cdot 10^4\ cm/s$. It is possible that in a real MC the value of S_0 could be 100 times smaller [9].

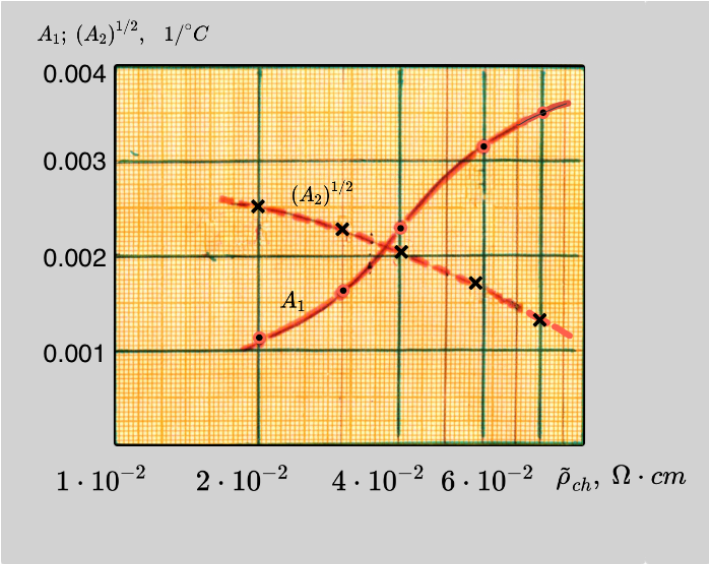

Figure 23. Dependences of approximation coefficients of temperature dependences of input resistance on average resistivity PCH, obtained from the research of diffusion channels PCH.

To determine the values of the approximation coefficients of the temperature dependences of the sensitivity coefficients K_A, K_B, K_C and resistance A_1, A_2 at the previously selected values of the average resistivity of the diffusion alloyed samples PCH with structure $MS\#7$ were made. The experimentally obtained dependences of the coefficients in the $\tilde{\rho}_{ch} = (2 \div 8) \cdot 10^{-2}\ \Omega \cdot cm$ dianazone are shown in Fig.23 and Fig.24.

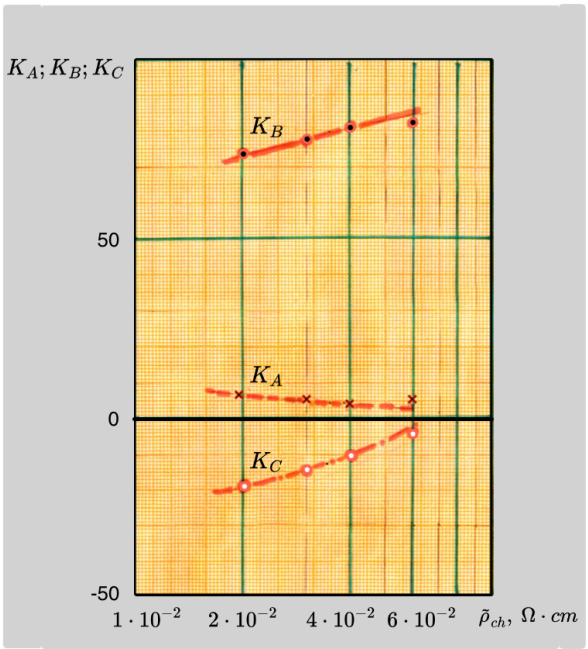

Figure 24. Dependences of the $K_A; K_B; K_C$ approximation coefficients of the temperature dependences of the strain sensitivity PCH on the average resistivity PCH $\tilde{\rho}_{ch}$, obtained from the research of the diffusion channels PCH.

The approximation coefficients of the ion-doped PCH were experimentally measured using IPT with the topological structures MC discussed in the table.

Based on the results of statistical processing of measurements on undivided silicon wafers, the smallest scatter of input resistances R_{in}, less than $\pm 2.5\%$ and normalized null output K_{mc0} less than $\pm 1.2\ mV/V$ are determined for $MC\#7$
and $MC\#10$. These structures are also characterized by the lowest average values of K_{mc0}, equal to $+1.2\ mV/V$ and $-1.2\ mV/V$, respectively. The values of the approximation coefficients of the temperature dependences of the sensitivity and resistance for topological structures MC with ion alloyed PCH are given in Table 4.1.

Table 4.1. Values of approximation coefficients of test-IPT with ion-doped PCH

	K_A	K_B	K_C	$\mathrm{A}_1, 1/\mathrm{K}$	$\mathrm{A}_2, 1/\mathrm{K}^2$
$\#4$	$10 \pm 5\%$	$60 \pm 8\%$	$-(14 \pm 25\%)$	$(1.14 \pm 0.03) \cdot 10^{-3}$	$(1.5 \pm 0.4) \cdot 10^{-6}$
$\#10$	$5 \pm 2\%$	$60 \pm 7\%$	$-(16 \pm 25\%)$	$(1.14 \pm 0.03) \cdot 10^{-3}$	$(1.5 \pm 0.4) \cdot 10^{-6}$

2. Monolithic IPT with Distributed Parameters

A characteristic feature of the monolithic IPT design with distributed parameters is the electrical connection of the volume of the elastic element to MC by redistribution of the charge carrier current in PCH and EE. For this purpose, the PCH and contact regions are formed by locally doping the impurity that increases the concentration level of the majority charge carriers in the elastic element of silicon, for example, in EE of silicon type P by ion implantation or diffusion of boron.

As shown in Chapter 2, the redistribution effect of charge carrier current in MC begins to show in the characteristics when the resistivities of the elastic element of silicon $\rho_{ee} < 20\ \Omega \cdot cm$. For this case, the design parameters IPT, where $\frac{H_{ee}}{a} \geqslant 0.3$, can be found from relations (3.14), (3.17) and (3.18):

$$\frac{V_{out}^{dp}(T)}{V_{\text{in}}} = \frac{R_2(T)}{R_1(T) + R_2(T) + 9.1 \cdot 10^{-3} \cdot \frac{R_1(T) \cdot R_2(T)}{\rho_{ee}(T)}} - \frac{R_3(T)}{R_4(T) + R_3(T) + 9.1 \cdot 10^{-3} \cdot \frac{R_3(T) \cdot R_4(T)}{\rho_{ee}(T)}} \tag{60}$$

$$K_{mc}^{dp} = \frac{K_{ch}(T)}{1 + 4.55 \cdot 10^{-3} \cdot \frac{R_{ch}(T)}{\rho_{ee}(T)}} \tag{61}$$

$$R_{in}^{dc} = \frac{R_{ch}(T)}{\frac{2 + 18.2 \cdot 10^{-3} \cdot \frac{R_{ch}(T)}{\rho_{ee}(T)}}{2 + 9.1 \cdot 10^{-3} \cdot \frac{R_{ch}(T)}{\rho_{ee}(T)}} + 0.707 \cdot \frac{R_{ch}(T) \cdot H_{ef} \cdot b}{\rho_{ee}(T) \cdot a}} \tag{62}$$

To confirm the calculation ratios obtained, to determine the design constraints for the placement of MC in the body EE and the pressure range of the working temperatures, a design of a pressure test transducer with a beam elastic element 5E.2251.205.00.00.000 was developed. The topological structure and geometric parameters are shown in Fig.25. The coordinates of the location MC in the volume EE relative to the x and y axes are changed by aligning the topological layers with specially formed signs in the oxide layer of the silicon plate. This solution significantly simplified the design of the test transducer and reduced the error in reproducing the specified geometric dimensions of the bridge circuit.

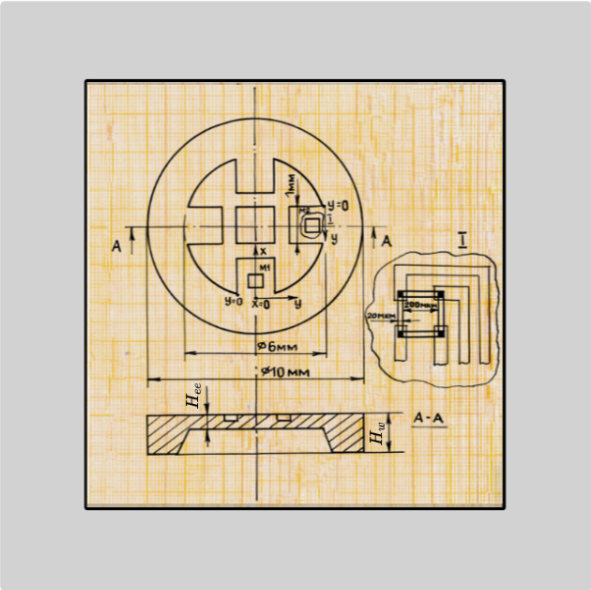

Figure 25. Topological structure and geometrical parametries
Test-IPT pressure with distributed parameters
5.EH.2251.205.00.00.000.

The model samples of IPT were made from silicon wafers $KDB-0.5(P-Type\ 0.5\ \Omega\cdot cm)$, $KDB-10(P-Type\ 10\ \Omega\cdot cm)$, $KDB-4.5(P-Type\ 4.5\ \Omega\cdot cm)$, using boron ion implantation with a doping dose of $2\cdot 10^{15}cm^{-2}$ to form PCH (with a sheet resistance of $R_{Sch}=85\ \Omega/\square$). IPT with elastic elements of N-type silicon wafers $KEF-4.5(N-Type\ 4.5\Omega\cdot cm)$ and an insulating p-n junction are intended to determine the parameters if PCH is electrically isolated (these are R_{ch} and K_{ch}

To calculate the IPT parameters, the following input data were used:

- temperature variations of the specific resistance $\rho_{ee}(T)$ up to the temperature of intrinsic conductivity obtained from the temperature dependencies of the differential temperature coefficients of specific resistance $\alpha_{\rho_{ee}}=\frac{1}{\rho_{ee}(T)}\frac{d\rho_{ee}(T)}{dT}$, calculated in [14] for uniformly doped layers of p-type silicon:
  for $\rho_{ee1}=0.5\ \Omega\cdot cm\ (KDB-0.5)$
  $$\rho_{ee1}(T)=0.5\left[1+6.6\cdot 10^{-3}(T-T_0)+1.4\cdot 10^{-5}(T-T_0)^2\right];$$
  for $\rho_{ee2}=1\ \Omega\cdot cm\ (KDB-1)$
  $$\rho_{ee2}(T)=1+7.6\cdot 10^{-3}(T-T_0)+1.6\cdot 10^{-5}(T-T_0)^2;$$
  for $\rho_{ee1}=10\ \Omega\cdot cm\ (KDB-10)$
  $$\rho_{ee3}(T)=10\left[1+7.83\cdot 10^{-3}(T-T_0)+1.68\cdot 10^{-5}(T-T_0)^2\right];$$
- values of the temperature of intrinsic conductivity T_{int}, calculated in [10] ($\alpha_{\rho_{ee}}=0$):

#	Resistivity	Intrinsic Conductivity Temperature
1	ρ_{ee_1}	$325^\circ C$
2	ρ_{ee_2}	$300^\circ C$
3	ρ_{ee3}	$200^\circ C$

- temperature variations of the resistance R_{ch} and the gauge factor K_{ch} of electrically isolated ion-implanted PCH, determined in Chapter 4 (see Table 4.1).
- effective thickness H_{ef} determined from the graph in Fig.17, under the condition of appearance of the input resistance MC dependence on the thickness EE (H_{ee}, $\frac{H_{ee}}{a}\leqslant 0.3$) for IPT $5.EH.2251.205.00.00.000$, where $a=200\cdot 10^{-4}\ cm$, equal to $H_{ef}=60\cdot 10^{-4}\ cm$;

- allowable variations of IPT parameters when changing the location of MC for the normalized null output $\Delta K_{mc0} \leqslant \pm 0.2 \frac{mV}{V}$ and the temperature instability coefficient of the normalized null output $\Delta \gamma_{mc0} \leqslant \pm 0,01\ \%/^{\circ}C$.

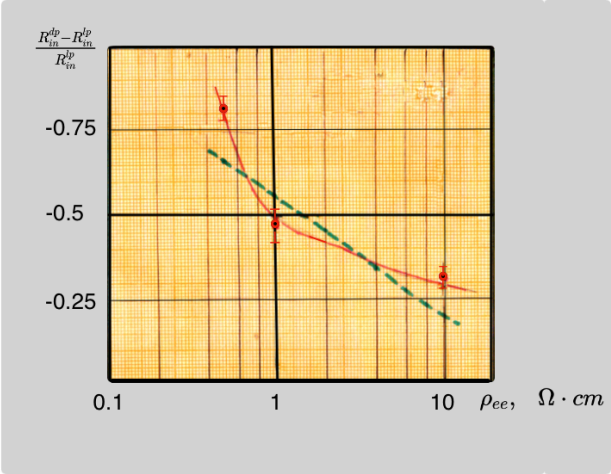

Figure 26. Dependences of variations of input resistance of MC with distributed parameters R_{in}^{dp} relative to its value for isolated R_{in}^{lp} on the resistivity EE

calculated experimental

The calculated and experimental dependencies of changes in the input resistance MC relative to its value for electrically insulated PCH on the specific resistance EE are shown in Fig.26. Differences in dependencies for specific resistances ρ_{EE} in the range of $(0.6 \div 10)\ \Omega \cdot cm$ do not exceed $\pm 10\%$. A more precise match is observed between the calculated and experimental dependencies for changes in the piezoresistive coefficient $K_{mc}(\rho_{ee})$ in Fig.27.

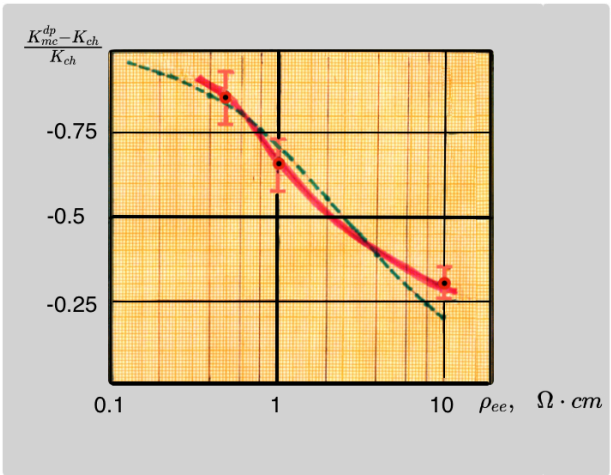

Figure 27. Dependences of variations of strain factor of MC with distributed parameters K_{mc}^{dp} relative to its value for isolated K_{ch} on the resistivity EE

calculated experimental

The graphs of changes in the magnitude of K_{mc0} and the temperature coefficient of instability γ_{mc0} of the normalized null output MC depending on the location of the circuit in the beam EE with a thickness of $H_{ee} = 100 \cdot 10^{-4}\ cm$ are shown in Fig.28. Changes in the parameters of IPT (with a possible redistribution of the charge carriers' current in the volume of the rigid base with a thickness of $H_w = 400 \cdot 10^{-4}\ cm$) are insignificant when MC approaches the rigid base (along the axis). This confirms the design limitation adopted in Chapter 3 $\frac{H_{ee}}{a} \leqslant 0.3$. The permissible approach of MC to the edge of EE $y = 0$ along the y axis in the graphs in Figs.28 (a)

and (b) is determined by the distance $\Delta L_y = 200\ \mu$. With further approach, when $\Delta L_y < 200\ \mu$, a significant change in parameters is observed, probably due to a change in the current redistribution in EE outside of the area limited by the channels of MC.

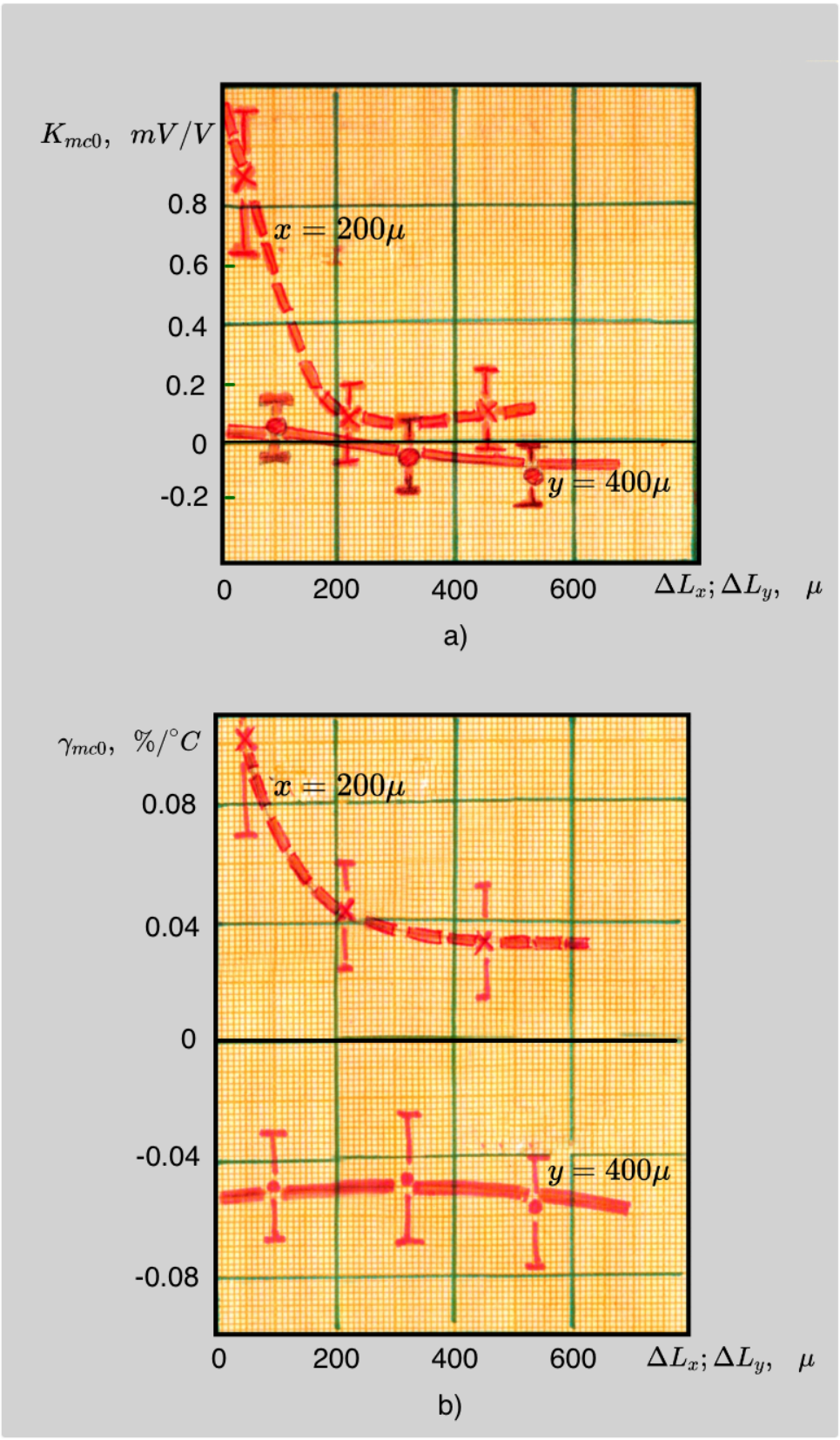

Figure 28. Graphs of changes in the magnitude K_{mc0} (a) and temperature instability coefficient γ_{mc0} (b) of the initial transfer coefficient of the MO

instability coefficient γ_{mc0} (b) of the initial transfer coefficient of the MC depending on the arrangement of the circuit on the elastic element.

Fig.29 shows the temperature changes calculated and experimentally obtained in the piezoresistive coefficients for IPT with specific resistances EE of $0.5\ \Omega \cdot cm$, $1\ \Omega \cdot cm$, $10\ \Omega \cdot cm$. The temperature ranges of operation for IPT are determined from the graphs as follows:

#	Resistivity	Operating Temperature Ranges
1	$\rho_{ee_1} = 0.5\ \Omega \cdot \text{cm}$	$(0 \div 325)^{\circ}\text{C}$
2	$\rho_{ee_2} = 1\ \Omega \cdot \text{cm}$	$(0 \div 300)^{\circ}\text{C}$
3	$\rho_{ee3} = 10\ \Omega \cdot \text{cm}$	$(-60 \div +200)^{\circ}\text{C}$

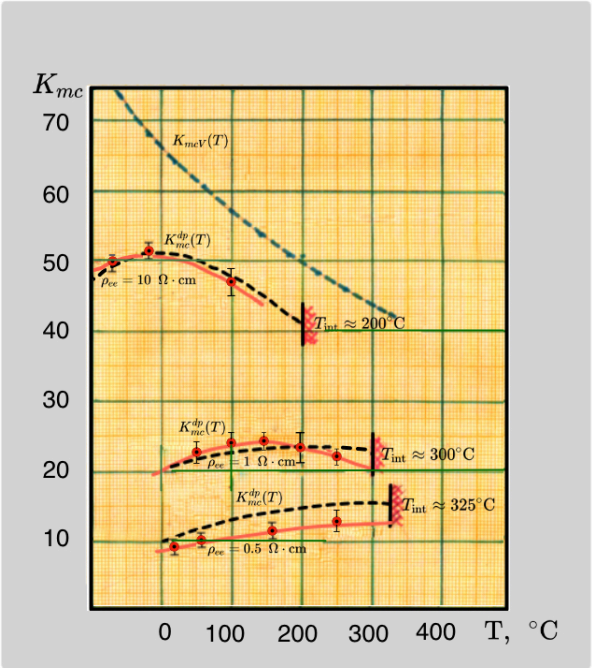

Figure 29. Calculated (----) and experimentally obtained (——) temperature changes of the strain-sensitivity coefficients for the IPT with spaced parameters $(K_{mc}^{dp}(T))$ and electrically isolated from the elastic element $(K_{mcV}(T))$

3. Study of Methods to Minimize the Intrinsic and Temperature Errors IPT

As shown in Chapter 1, the systematic component of the intrinsic error $\delta_{k_{ee}}$ for microinertial IPTs with $H_{ee} < 100 \cdot 10^{-4}\ cm$, which is associated with the reproducibility of the transformation characteristic under the technological dispersion of geometric sizes EE, can reach values up to $\delta_{k_{ee}} = \pm 40\%$. In this case, for low-frequency accelerometers with an intrinsic error of 5%, assuming that the error of modern low-frequency vibration measurement devices is $\pm 3\%$, the error value should not exceed $\pm 3\%$ [11] [12], and the yield of acceptable products in serial production should be less than 5%.

The identity of the conversion characteristic slope is achieved by additional adjustment with internal adjustment elements [13] [14]. However, most known adjustment methods have their drawbacks: they change the electrical

parameters of the sensor and limit the range of operating temperatures to values of $(+100 \div +150)^{\circ}C$.

A method for adjusting beam transducers for inertial action low-frequency accelerometers has been developed and studied by changing the conversion coefficient $EE\ K_{ee}$ [15]. The adjustment method is carried out as follows (see Fig.30): by anisotropic etching of the silicon wafer on the flat side elastic elements and inertial mass regions are formed. By anisotropic etching of the wafer on the flat side the EE regions are divided into groups of parallel bands with piezoresistors D_1 and regulating n bands D_2 without piezoresistors. The control of the parameters marked on the IPT wafer determines the systematic error component $\delta_{k_{ee}}$ and the resonance frequency f_0 [16]. To adjust, it is necessary to determine the total width value of the adjustable strips $m \cdot D_2$, which can be expressed by the equation:

$$m \cdot D_2 = \delta_{k_{ee}} \cdot (2 \cdot D_1 + n \cdot D_2) \qquad (63)$$

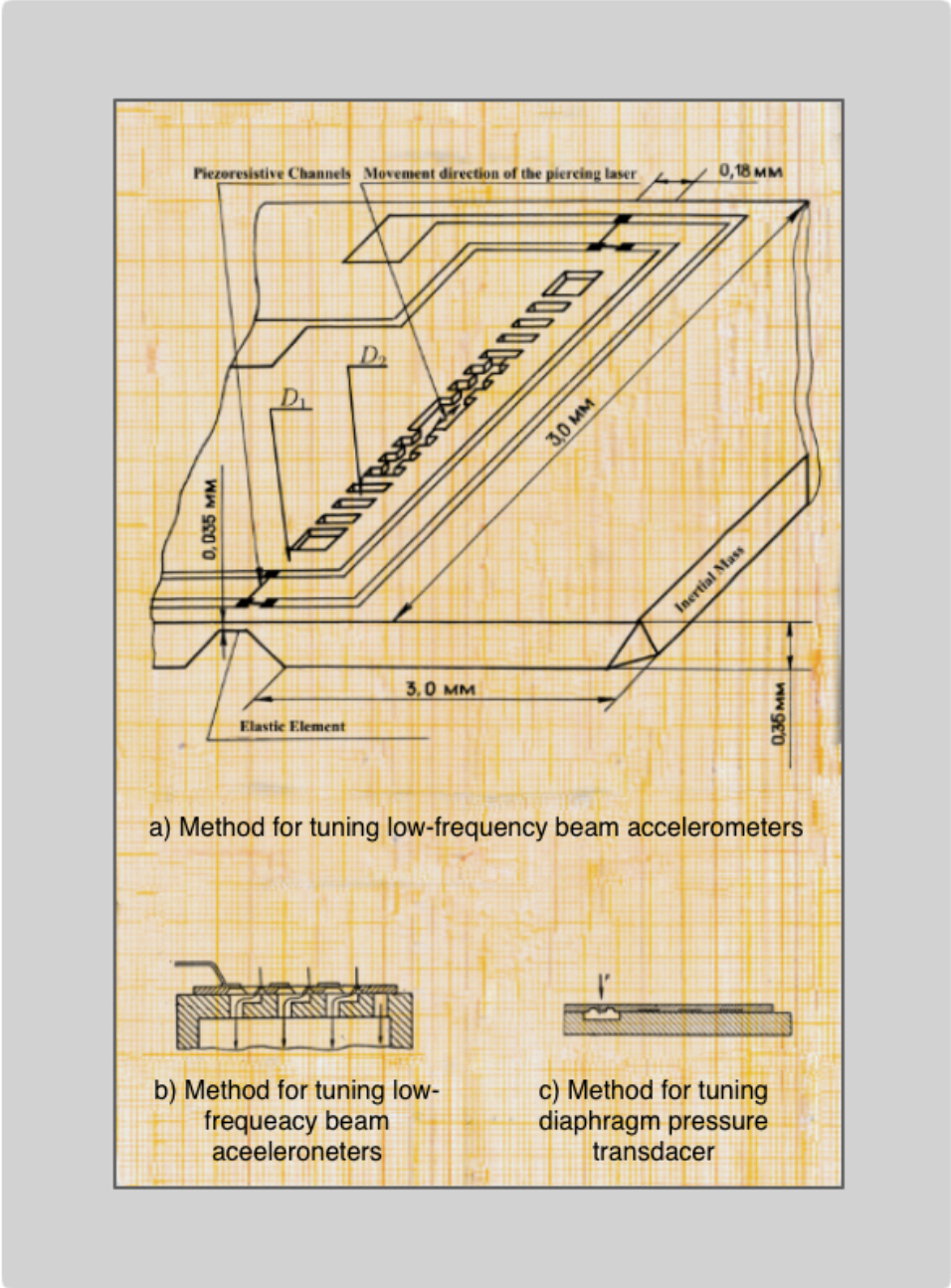

Figure 30. Tuning methods for integral piezoresistive transducers (IPT)

Then m adjustment strips are torn without violating the symmetry of the elastic element. For the design of a low-frequency accelerometer SIAP 402.139.001, where

$$D_1 = 400 \times 10^{-4}\ \text{cm}, \quad D_2 = 40 \times 10^{-4}\ \text{cm}, \quad n = 32,$$

the required number of tear strips is determined by the equation:

$$m = \delta_{k_{ee}} \frac{2 \cdot D_1 + n \cdot D_2}{D_2} = 52 \cdot \delta_{k_{ee}} \qquad (64)$$

The following results were obtained during the tuning of the low-frequency accelerometers:

Transducer Number	Sensitivity Before Tuning mV/g	Required Sensitivity mV/g	$\delta_{k_{ee}}$	m	Sensitivity After Adjustment mV/g
1	10.2	15	33%	18	15.3
2	7.9	10	21%	12	10.2
3	13.2	15	12%	6	14.6

Adjusting the slope of the transfer characteristic of the membrane pressure sensors, where the intrinsic error should not exceed $\pm 1\%$, is carried out by changing the thickness during transducer formation [17].

Periodically, during pauses in the etching process, the silicon plate with the IPT is placed on a probe set-up, a control transducer (one or more) is loaded with a constant mechanical value, and the output electrical signal is measured. Etching is stopped when the desired output signal is reached.

Advantages of the methods considered: electrical parameters and the working temperature range of the sensor remain unchanged; the output of usable parts increases by more than 10 times; the systematic component of the intrinsic error decreases by more than 10 times.

3.1. Monolithic IPT with a p-n junction isolating the measurement circuit

Based on the results of studies of temperature changes in normalized null output K_{mc0}, the additive component of the additional temperature error is determined by the value of $\gamma_0 \leqslant 0.04\ \%/^\circ C$. The standard value of the additive temperature error for pressure sensors with an intrinsic error of $\pm 1\%$ is $0.06\%^\circ C$ (for low-frequency accelerometers with an intrinsic error of $\pm 5\%, 0.1\%^\circ C$). Thus, the allowable value of the multiplicative error component during temperature changes in bridge sensitivity $K_{mcV}(T)$ should be $\gamma_{mc} = 0.04\%^\circ C$ ($\gamma_{mc} = 0.07\%^\circ C$ for accelerometers). The error parameter γ for the temperature range (T_1, T_2) is estimated by the change in the output signal as a percentage of its nominal value when the ambient temperature changes (the temperature instability of the output signal) [1:2] [2:1]:

$$\frac{V_{out_{max}} - V_{out_{min}}}{V_{out}(T_0)} \cdot \frac{1}{T_2 - T_1} \cdot 100\% \leq \gamma;\ \%/^\circ C \quad (65)$$

where $V_{out_{max}}$ and $V_{out_{min}}$ are the maximum and minimum values of the output signal when the temperature changes.

When analyzing the conditions for implementing compensation for changes in temperature in the conversion characteristic (multiplicative component), the differential temperature coefficient of sensitivity [18] is used, which is equal to

$$\Gamma_{mc} = \frac{1}{K_{mc}(T)} \cdot \frac{dK_{mc}(T)}{dT} \qquad (66)$$

where $K_{mc} = \frac{1}{V_{in}(T)} \frac{dV_{out}(T)}{dT}$ is the MC sensitivity IPT.

The temperature dependence of the characteristics of the conversion with an isolated p-n junction in the case of providing the MC from a stabilized voltage source ($V_{in} = V_{input} = const$) is characterized by the coefficients obtained from relations (19) and (39), provided that $K_{\parallel} = -K_{\perp}$, as follows:

$$\Gamma_{mcV} = \Gamma_{V2} \left(\frac{T_0}{T} \right)^2 + \Gamma_{V3} \left(\frac{T_0}{T} \right)^3 \qquad (67)$$

where

$$\Gamma_{V2} = -\frac{K_B}{T_0\left[K_A + K_B\frac{T_0}{T} + K_C\left(\frac{T_0}{T}\right)^2\right]}; \quad (68)$$

$$\Gamma_{V3} = -\frac{2K_C}{T_0\left[K_A + K_B\frac{T_0}{T} + K_C\left(\frac{T_0}{T}\right)^2\right]}, \quad (69)$$

then

$$\Gamma_{mcV} = -\frac{K_B\cdot\left(\frac{T_0}{T}\right)^2 + 2K_C\cdot\left(\frac{T_0}{T}\right)^3}{T_0\cdot\left[K_A + K_B\cdot\frac{T_0}{T} + K_C\cdot\left(\frac{T_0}{T}\right)^2\right]} \quad (70)$$

The compensation condition for the temperature dependence of the conversion characteristics is possible at $T = T_0$ if $K_B = K_C = 0$ (a) or $K_B = -2K_C$ (b). Condition (a) for PCH diffusion is expected at $\rho_{ee} < 1 \cdot 10^{-3}\ \Omega \cdot cm$, but due to physical limitations in the form of the maximum solubility of boron, it is not achievable. Condition (b) is not realized (as can be seen from the graph in Fig.24). Similar conclusions apply to IPT with PCH implanted with ions (see Table 4.1). The minimum calculated values of γ obtained from the experimental data of the graph in Fig.24 and in Table 4.1 are: for diffusion channels $0.13\%^{\circ}C$, for ion-implanted channels $0.12\ \%/^{0}C$.

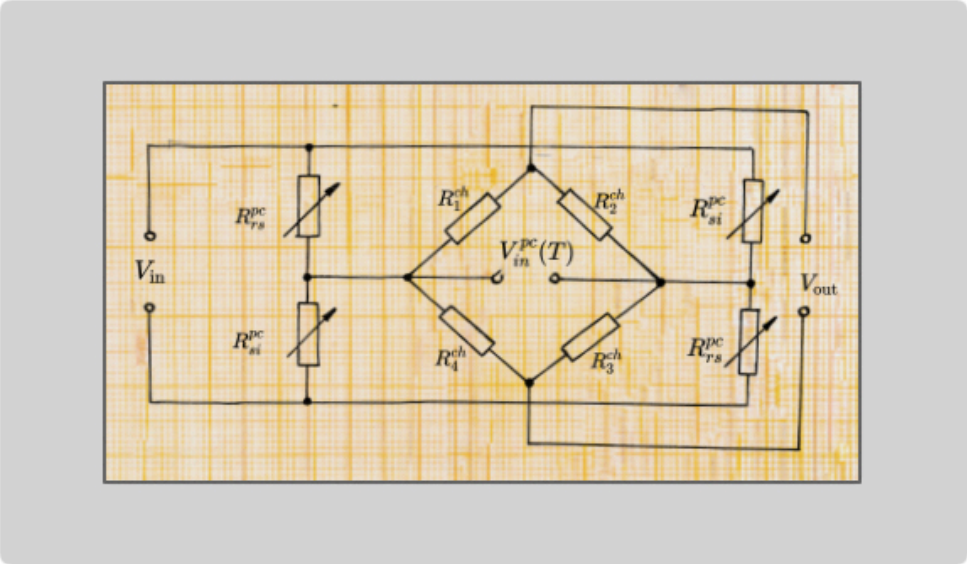

Figure 31. IPT wiring diagram with TCC

To create sensors with low γ values, it is necessary to use a thermal compensation circuit (TCC). The studied TCC design contains trim resistors with different signs of TCR. Fig.31 shows the circuit IPT with TCC, where R_{rs}^{tc} is the thin film trimming resistor made of RS-1004 material, R_{si}^{tc} is the silicon diffusion trimming resistor with $\tilde{\rho}_{si} = 7 \cdot 10^{-2}\ \Omega \cdot cm$. The choice of resistive elements TCC is due to the fact that RS1004 thin film resistors and diffusion resistors retain their characteristics in the same temperature range as $PCH\ IPT$, that is, $(0 \div +230)^{0}C$. The experimental dependence of the temperature change of thermoresistors based on RS-1004 material applied to silicon substrates has been established [19] [20] [15:1]:

$$R_{rs}^{tc}(T) = R_{rs0}^{tc} \cdot \left[1 - 2.7 \cdot 10^{-3}\,(T - T_0) + 7.3 \cdot 10^{-6}(T - T_0)^2\right] \quad (71)$$

The experimental temperature dependence for the diffusion resistor R is as follows:

$$R_{si}^{tc}(T) = R_{si0}^{tc} \cdot \left[1 + 3.4 \cdot 10^{-3}\,(T - T_0) + 2.3 \cdot 10^{-6}(T - T_0)^2\right] \quad (72)$$

The transformation function of the IPT with TCC input mechanical value ε_{x_0} into the output electrical signal V_{out} is determined by the relationship:

$$V_{out}(T) = V_{in}(T) \cdot K_{mc}(T) \cdot \varepsilon_{x_0} = V_{input} \cdot K_{tc}(T) \cdot K_{mc}(T) \cdot \varepsilon_{x_0} \quad (73)$$

$K_{tc}(T)$ is the coefficient of transformation of the stabilized voltage of the source V_{input} into the temperature-dependent power supply voltage $MC\,V_{in}(T)$.
For the IPT circuit in Fig.31 from [21], the conversion coefficient is equal to:

$$K_{tc}(T) = \frac{V_{in}(T)}{U_{input}} = \frac{R_{si}^{tc}(T) - R_{rs}^{tc}(T)}{R_{rs}^{tc}(T) + R_{si}^{tc}(T) + 2\frac{R_{rs}^{tc}(T) \cdot R_{si}^{tc}(T)}{R_{in}(T)}} \quad (74)$$

If the temperature dependence $K_{mc}(T)$ is defined by a second degree polynomial (19), then the conversion function (73) for the IPT circuit with TCC in Fig.31 is:

$$V_{\text{out}}\,(T) = V_{\text{input}}\ \cdot \varepsilon_{x_0} \cdot \frac{\left[R_{si}^{tc}(T) - R_{rs}^{tc}(T)\right] \cdot \left[K_A + K_0\frac{T_0}{T} + K_C\left(\frac{T_0}{T}\right)^2\right]}{R_{rs}^{tc}(T) + R_{si}^{tc}(T) + 2 \cdot \frac{R_{rs}^{tc}(T) \cdot R_{si}^{tc}(T)}{R_{\text{in}}\,(T)}} \quad (75)$$

Given relations (67), (73) and (74), the differential temperature sensitivity coefficient for IPT with TCC, from (66) is

$$\Gamma_{mcV}^{tc} = \frac{dK_{tc}(T)}{K_{tc}(T)dT} + \Gamma_{mcV} \quad (76)$$

The design of a beam force transducer 5E.2251.130.00.00.000 (see Fig.18) was selected for the calculation and modeling of the IPT circuit with TCC. The input resistance of IPT with ion-implanted PCH at $T = 25^{\circ}C$ is $R_{in} = 1000\ \Omega$. Taking into account the parameters in Table 4.1, the temperature changes of $R_{in}(T)$ are determined by the experimentally obtained dependence:

$$R_{in}^{bc}(T) = R_{in0}^{bc}\left[1 + 1.1 \cdot 10^{-3}\,(T - T_0) + 1.5 \cdot 10^{-6}(T - T_0)^2\right] \quad (77)$$

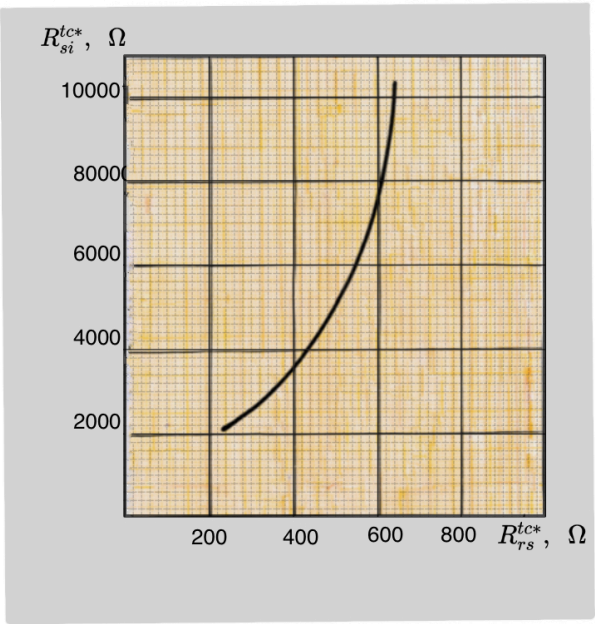

Figure 32. Calculated graph of resistance values TCC providing thermal compensation condition at temperature $T = T_0 = 150^{\circ}\text{C}$.

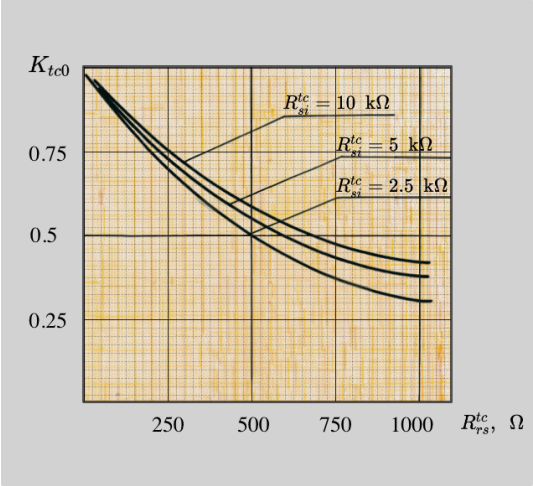

Figure 33. Calculated graph of K_{tc0} values for different values of R_{rs}^{tc}, R_{si}^{tc}

The values of the parameters R_{rs}^{tc*}, R_{si}^{tc*}, and K_{tc0}^{*} under normal conditions ($T = 25°C$) that provide thermocompensation $\Gamma_{mcV}^{tc} = 0$ at temperature $T = T_0 = 150°C$ are determined by the "golden section" method of minimization [22]. Fig.32 shows the calculated graph of TCC resistance values that satisfy the condition $\Gamma_{mcV}^{tc} = 0$ at temperature $T = T_0 = 150°C$. From equation (73) and the graph in Fig.33, which presents the calculated values of K_{tc0} for different values of R_{rs}^{tc}, R_{si}^{tc}, it can be seen that when using TCC containing adjustment resistors with TCR of different signs, the sensitivity of IPT decreases by 1.5 2 times. The calculation of IPT design using the methodology proposed in [75]shows that the connection of TCC as shown in the figure allows the design of compact low-frequency accelerometers to measure accelerations of $0 \pm 1g$ in the frequency range of $0 \div 100\ Hz$. The figure shows the experimentally obtained temperature dependencies of the sensitivity changes for the force test IPT with and without compensation in the temperature range of $(0 \div +230)°C$. Connecting TCC containing adjustment resistors with different TCR signs reduced the parameter γ from $0.13\ \%/°C$ to $0.015\ \%/°C$ (see Fig.34).

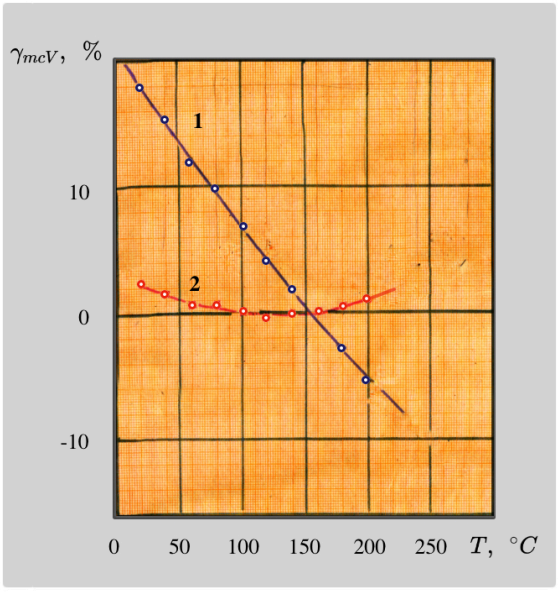

Fugure 34. Temperature dependences of the coefficient γ_{mcV} when supplied powered from a stabilized voltage source:1- IPT without compensation circuit; 2 - IPT with TCC containing regulating resistors with TCR of different sign.

In articles [23] [24] [25], the results of research on the physical and functional models of the IPT with an isolating $p-n$ junction are presented for the case of powering the MC from a stabilized current source in the temperature range of $(-60 \div +80)^{\circ}C$. When analyzing the conditions to implement compensation for temperature changes in the conversion characteristic, the differential temperature sensitivity coefficient [18:1] is used, which is given by

$$\Gamma mcI = \frac{1}{KmcI_0}\frac{dK_{mcI}(T)}{dT}, \qquad (78)$$

where

$$K_{mcI}(T) = \frac{V_{out}(T)}{I_{in}\cdot\varepsilon_{x_0}} = R_{in_0}\cdot\left[1 + A_1\cdot(T-T_0) + A_2\cdot(T-T_0)^2\right]\times$$

$$\times\left[K_A + K_B\cdot\frac{T_0}{T} + K_C\cdot\left(\frac{T_0}{T}\right)^2\right]$$

is the sensitivity coefficient of the MC when supplied with a stabilized current.

The differential temperature sensitivity coefficient for this case is given by:

$$\Gamma_{mcI} = \Gamma_{I0} + \Gamma_{I1}\cdot T + \Gamma_{I2}\cdot\left(\tfrac{T_0}{T}\right)^2 + \Gamma_{I3}\cdot\left(\tfrac{T_0}{T}\right)^3 \quad (79)$$

where

$$\Gamma_{I1} = 2\cdot\tfrac{K_A\cdot A_2}{K_A+K_B+K_C} \qquad (80)$$

$$\Gamma_{I2} = \tfrac{K_B\left(A_1 - A_2\cdot T_0 - \frac{1}{T_0}\right) - K_C\cdot(A_1 - 2A_2\cdot T_0)}{R_A+R_B+R_C} \qquad (81)$$

$$\Gamma_{I3} = 2\cdot\tfrac{K_B\cdot\left(A_1 - A_2\cdot T_0 - \frac{1}{T_0}\right)}{K_A+K_B+K_C} \qquad (82)$$

The choice of optimal average resistivity values in the range of $\tilde{\rho}_{ch} = \left(2\cdot10^{-2} \div 8\cdot10^{-2}\right)\ \Omega\cdot cm$ determines the conditions for the IPT compensation in the temperature range of $(0 \div +300)^0C$ [18:2]. For the given values of $\gamma_{mc} \leqslant 0.04\%/^0C$, the temperature working ranges for IPT with an isolated p-n junction are given in Tables 4.2 and Table 4.3.

Table 4.2 IPT with lumped parameters for diffusion channels

#	Resistivity	Operating Temperature Ranges
1	$\tilde{\rho}_{ch1} = 3\cdot10^{-2}\Omega\cdot\text{cm}$	$(-20 \div +180)^0\text{C}$
2	$\tilde{\rho}_{ch2} = 3.5\cdot10^{-2}\Omega\cdot\text{cm}$	$(0 \div +210)^0\text{C}$
3	$\tilde{\rho}_{ch3} = 4\cdot10^{-2}\Omega\cdot\text{cm}$	$(+50 \div +210)^0\text{C}$

Table 4.3 IPT with lumped parameters for Ion-alloyed channels

#	Dose of doping	Operating Temperature Ranges
1	$N_{id} = 2\cdot10^{15}\ \text{cm}^{-2}$	$(+50 \div +210)^0\text{C}$

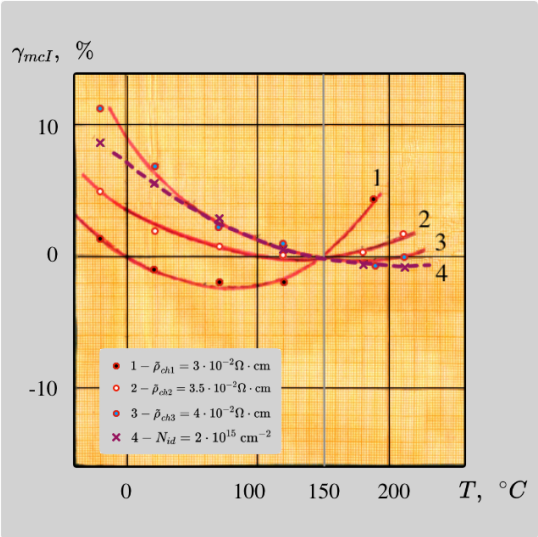

Figure 35. Temperature dependences of the sensitivity coefficient K_{mcI} when powered from a stabilized current source for the MC:
with diffusion channels
with ion-alloy channels

Fig.35 shows the experimentally obtained temperature dependences of the sensitivity change for the IPT without TCC with a power supply of the measuring circuit from a stabilized current source. For IPT with ion-alloyed PCH at a dose of $2 \cdot 10^{15}\ cm^{-2}$, the temperature range is defined from 0 °C to 210 °C.

3.2. Monolithic IPTs with distributed parameters without insulating p-n junction

One significant difference in the construction of a distributed parameter IPT is the electrical connection of the elastic element to the measurement circuit. In such a design, the elastic element is not only a converter of mechanical quantity into deformation, but also a means of regulating the temperature dependence of the output signal with precise information about changes in the ambient temperature, as it combines the functions of heat transfer on the sensor's PCH. This design increases the reliability of the sensor at high temperatures above $+200^{\circ}C$ since it does not require any elements to adjust its characteristics, and the parametric failure of the elastic element can occur only simultaneously with its mechanical failure.

Determining the compensation conditions $\Gamma_{mc}^{dp} = 0$ for a distributed parameter IPT is a complex technical task related to the optimal selection of various design and technological parameters: specific resistance of the elastic element, average specific resistance of the PCH, thickness of the elastic element, geometric dimensions and shape of the topological structure of IPT', etc. In this case, we consider the sensor's construction described in Section 3.2.

When powering the distributed parameter sensor from a stabilized voltage source, the differential temperature coefficient of the sensitivity, taking into account the empirical temperature dependencies of $K_{mc}(T)$ and $R_{ch}(T)$ and the relationships (61) and (66), is equal to:

$$\Gamma_{mc}^{dp} = \Gamma_{mcV} - \frac{\Lambda \cdot \left[\frac{A_1^{ch} + 2A_2^{ch} \cdot (T - T_0)}{1 + A_1^{ch} \cdot (T - T_0) + A_2^{ch} \cdot (T - T_0)^2} - \frac{A_1^{ee} + 2A_2^{ee} \cdot (T - T_0)}{1 + A_1^{ee} \cdot (T - T_0) + A_2^{ee} \cdot (T - T_0)^2} \right] \cdot \frac{R^{ch}(T)}{\rho_{ee}(T)}}{2 + \Lambda \cdot \frac{R^{ch}(T)}{\rho_{ee}(T)}} \quad (83)$$

where

$$\Gamma_{mcV} = -\frac{K_B \left(\frac{T_0}{T}\right)^2 + 2K_c \left(\frac{T_0}{T}\right)^3}{T_0 \left[K_A + K_B \frac{T_0}{T} + K_C \left(\frac{T_0}{T}\right)^2\right]} \quad (84)$$

differential temperature coefficient of strain-sensitivity for electrically isolated PCH with insulating $p-n$ junction. Operating temperature ranges for IPT with distributed parameters without isolating $p-n$ junction are presented in Table 4.4

Table 4.4 IPT with distributed parameters

#	Resistivity	Operating Temperature Ranges
1	$\rho_{ee_1} = 10\Omega \cdot \text{cm}$	$(-50 \div +200)^{\circ}\text{C}$
2	$\rho_{ee_2} = 1\Omega \cdot \text{cm}$	$(0 \div +300)^{\circ}\text{C}$
3	$\rho_{ee3} = 0.5\Omega \cdot \text{cm}$	$(0 \div +325)^{\circ}\text{C}$

The graph of Fig.36 shows the dependence of the temperature T_{tc}, when $\Gamma_{mc}^{dp} = 0$, on the specific resistance of the elastic element, calculated using formula (83) for the IPT design, in which PCH is formed by ion implantation of boron with a doping dose of $2 \cdot 10^{15}$ cm^{-2} and a parameter $\frac{H_{ee}}{a} \geq 0.3$. The graph of Fig.29 shows the calculated and experimentally obtained temperature dependences of the sensitive coefficient for designs with $\rho_{ee_2} = 1\Omega \cdot \text{cm}$, selected for the design of miniature pressure sensors. The parameter characterizing the additional temperature error in the temperature range $(0 \div 300)^{\circ}C$ is $\gamma_{mc} = 0.04\ \%/^{\circ}C$.

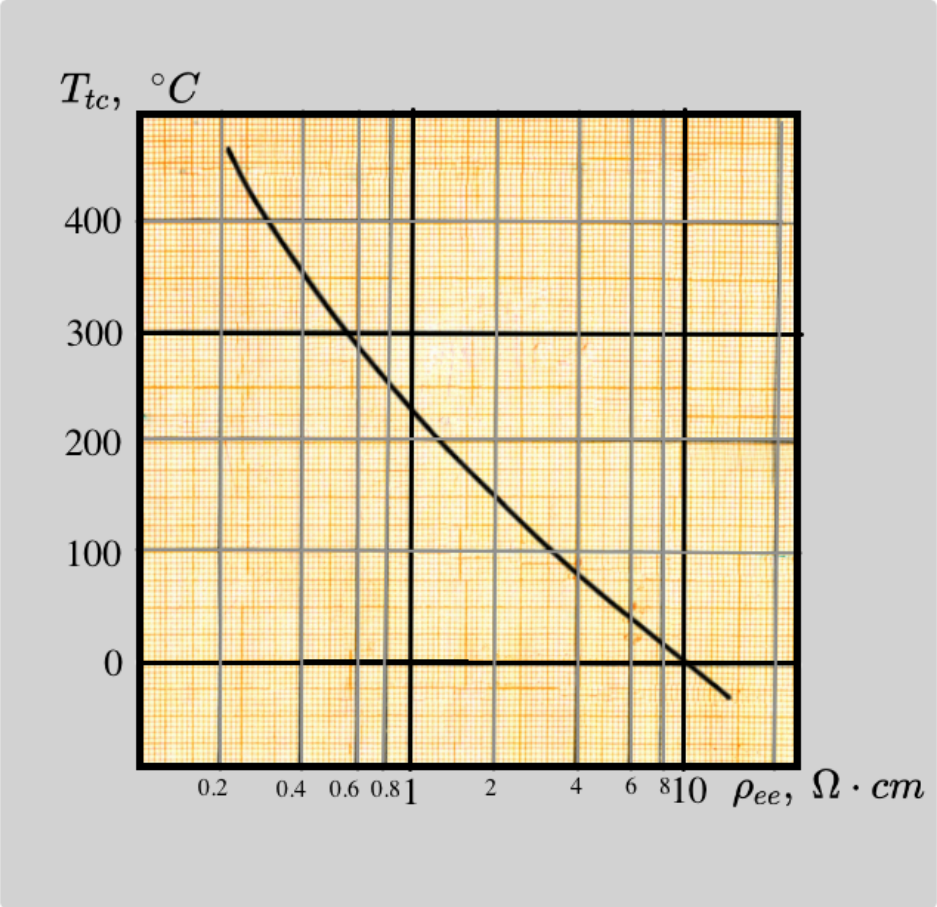

Figure 36. Calculated dependence of the temperature , when $\Gamma_{mc}^{dp} = 0$, on the resistivity of the elastic element for an IPT with distributed parameters, where PCHs are formed by ion implantation of boron

4. Conclusions

1. The influence of minimizing the geometric dimensions of monolithic IPTs with a total area of the isolating $p-n$ junction $A_{p-n}<2\cdot10^{-3}\ \text{cm}^2$ on the upper limit of the operating temperature range and the temperature dependence of the normalized null output MC has been studied. It has been experimentally confirmed that the upper limit of the operating temperature range depends on the design parameters: the perimeter-to-area ratio of the isolating $p-n$ junction K_{p-n} and the number of corners in the topological structure of p-type regions of MC, n_{p-n}. Provided that $A_{p-n}<2\cdot10^{-4}\ \text{cm}^2$, $K_{p-n}=500\div700$, $n_{p-n}\leqslant8$, the upper limit of the operating temperature range for IPTs with an isolating $p-n$ junction corresponds to $(+250\div300)^{\circ}C$.
2. The temperature changes of the electrophysical characteristics of PCH required for the creation of compact sensors with a range of operating temperatures up to $(+250\div300)^{\circ}C$ have been investigated. The experimental regular dependences of the approximation coefficients of temperature changes in deformation sensitivity by the polynomial of the second degree of the form $K_{mc}(T)=K_A+K_B\frac{T}{T_0}+K_C\left(\frac{T}{T_0}\right)^2$ and electrical resistance by the polynomial of the second degree of the form $R_{ch}(T)=R_{ch_0}\left[1+A_1\left(T-T_0\right)+A_2(T-T_0)^2\right]$. Approximation coefficients of temperature changes $K_{ch}(T)$ and R_{ch} for diffusional PCH with the average resistance of the material in the range $\tilde{\rho}_{ch}=\left(2\cdot10^{-2}\div8\cdot10^{-2}\right)\ \Omega\cdot cm$ and for boron implanted PCH with doping dose $2\cdot10^{15}\ cm^2$.
3. The electrical and constructional characteristics of IPT with distributed parameters were investigated to design small sensors with a working temperature range of $-60^{\circ}C$ to $325^{\circ}C$, where the construction parameter $\frac{H_{ee}}{a}\geqslant0.3$. The experimental dependencies of the sensitivity coefficient and input resistance of MC on the specific resistance of the material EE in the range of $\rho_{ee}=(0.1\div10)\ \Omega\cdot cm$ differ by no more than 10% from those calculated from the relations obtained during modeling in Chapter 2. The construction parameter ΔL, which determines the allowable approximation to the edge of EE, was experimentally determined to be $\triangle L\geqslant200\ \mu$. The working temperature ranges were determined based on the temperature changes of the electrical characteristics as follows:
$$\begin{aligned}\rho_{\text{ee }1}&=0,5\Omega\cdot\text{cm}\quad 0\div325^{\circ}\text{C}\\ \rho_{\text{ee }2}&=1\Omega\cdot\text{cm}\quad 0\div300^{\circ}\text{C}\\ \rho_{\text{ee }3}&=10\Omega\cdot\text{cm}\quad -60\div+200^{\circ}\text{C}\end{aligned}$$
4. To minimize the intrinsic error of small-sized sensors with a temperature working range of $(0\div300)^{\circ}C$, a tuning method has been developed and experimentally studied, in which the adjustment of the conversion characteristic of IPT is carried out by changing the conversion coefficient of EE. The advantages are as follows: the electrical parameters of MC and the temperature working range of the sensor are not changed; the systematic component of the intrinsic error is reduced more than 10 times.
5. The principles of minimization of additional temperature error of IPT with insulating $p-n$ junction are formulated:
   - for the case of sensor power supply from stabilized voltage source using experimentally obtained regular temperature changes of strain-sensitivity, input resistance MC, resistance of thin-film resistive elements made of $RS-1004$ material; developed thermal compensation scheme allowing IPT adjustment with high accuracy (less than $0.05\%/^0C$) in temperature range $(0\div300)^{\circ}C$
   - for the case of sensor feeding from stabilizing current source, using the regular temperature changes of electro-physical characteristics, the possibilities of "auto-thermal compensation" were investigated experimentally by using the selection of optimal values of specific resistance of material $(1\div5)\%$; the following temperature ranges of the sensors with intrinsic error $(1\div5)\%$ were determined for the design of sensors: with diffusion
     $\tilde{\rho}_{ch1}=3\cdot10^{-2}\Omega\cdot\text{cm}\qquad(-20\div+180)^0\text{C}$
     $\tilde{\rho}_{ch2}=3.5\cdot10^{-2}\Omega\cdot\text{cm}\qquad(0\div+210)^0\text{C}$
     $\tilde{\rho}_{ch3}=4\cdot10^{-2}\Omega\cdot\text{cm}\qquad(+50\div+210)^0\text{C}$
     with ion-doped boron implantation doping $2\cdot10^{15}\ cm^2\ (0\div300)^{\circ}C$.
6. The method of thermocompensation sensitivity is proposed and tested experimentally, when the element that adjusts the temperature dependence of the output signal IPT with distributed parameters are elastic elements with perfectly accurate information on the change in ambient temperature. Advantages of the method: high reliability in the range of high temperatures, because no additional regulating element is required, and parametric failure of the EE section is possible only simultaneously with its mechanical destruction.

References

1. *GOST 22520-85 Preobrazovateli davleniya, vakuuma i raznosti davlenii s ehlektricheskimi analogovymi vykhodnymi signalami, SSI. Obshchie tekhnicheskie kharakteristiki. [Pressure, vacuum and pressure difference transmitters with electrical analog output signals, SSI. General specifications.]*. (1986). (In Russian). https://docs.cntd.ru/document/1200023454
↩ ↩ ↩
2. *GOST 15077-78 Datchiki siloizmeritel'nye tenzorezistornye GSP. Obshchie tekhnicheskie usloviya. [Strain gauges strain gauge GSP. General specifications]*. (1978). https://files.stroyinf.ru/Data2/1/4293776/4293776163.pdf
↩ ↩
3. Borshchev, V. N., Demidova, V. A., Spalek, Y. M., & Kharenko, K. Y. (1983). Ehlektrofizicheskie kharakteristiki tenzorezistivnykh struktur, legirovannykh implantirovannym borom. [Electrophysical characteristics of tensoresistive structures alloyed with implanted boron.]. *Tekhnologiya. Tekhnologiya Priborostroeniya: Nauch.-Tekhn.Sb. TSNTI "Poisk,"* 2(8 In Russian), 71–80.
↩
4. Trutko, A. F. (1971). *Metody rascheta tranzistorov [Transistor Calculation Methods]*. Ehnergiya (In Russian).
↩
5. Vul, B. M., & Shotov, A. P. (1957). O kraevom proboe p-n perekhodov v germanii [On Edge Breakdown of P-N Junctions in Germanium]. *ZHTF (In Russian)*.
↩
6. Kulikovskii, K. L., & Kuper, V. Y. (1986). *Metody i sredstva izmereniya. [Methods and means of measurement.]*: *Vol. (In Russian)*. Ehnergoatomizdat.
↩
7. Fedorov, A. G., Spalek, Y. M., Tikhomirov, M. Y., & Borschev, V. H. (1988). Vliyanie napryazhenii, sozdavaemykh termicheskim okislom v kanale tenzorezistora kremnievogo integral'nogo preobrazovatelya mekhanicheokikh velichin na ego vykhodnoi signal [Influence of tensions created by thermal oxide in the channel of the silicon integral transducer of mechanical quantities on its output signal]. *Technology. Technology of Instrument Making: Collection of Scientific-Technical Documents /TsNTI "Poisk" (In Russian)*, 4(13), 48–49.
↩
8. Fedorov, A. G., Spalek, Y. M., Morozov, Y. M., Tikhomirov, M. Y., Malkov, J. V., Borschev, V. N. (1984). *Sposob izgotovleniya integral'nykh datchikov mekhanicheskokh velichin. [Method of manufacturing the integral sensors of mechanical quantities]. Certificate of state registration no.* 1067979 (Patent No. 1067979). Otkrytiya. Izobreteniya.- 1984 - Vyp.2 .- S.217.
↩
9. Stepanenko, I. P. (1980). *Osnovy mikroehlektroniki [Fundamentals of microelectronics]*: *Vol. (In Russian)*. Sovetskoe radio.
↩
10. Marchenko Aleksandr N. (1978). *Upravlyaemye poluprovodnikovye rezistory. [Controlled Semiconductor Resistors]*: *Vol. (In Russian)*. Energia.
↩
11. Iorish, YU. I. (1986). Standarty nuzhdaetsya v korrektirovke. [The standards need to be adjusted.]. *Pribory i Sistemy Upravleniya [Instruments and Control Systems.]*, 7(in Rissian), 15–16.
↩
12. *OST 92-4334-80. Preobrazovateli vibroizmeritel'nye p'ezoehlektricheskie. Obshchie tekhnicheskie usloviya. [Piezoelectric vibration measuring transducers. General specifications.]*. (1980).
↩
13. Vaganov, V. I. (1983). *Integral'nye tenzopreobrazovateli [Integral strain gauges]*: *Vol. (In Russian)*. Ehnergoatomizdat.
↩
14. Pivonenkov, B., Arkharova, L. G., & Markin, S. (1979). *Method of Tuning Integral Tensiometric Bridge Circuits* (Patent No. SU691682A1).
↩
15. Tikhomirov, M. Y., Spalek, Y. M., Pivonenkov, B. I., Zhelonkin, E. A., Arkharova, L. G., & Kolesnikov Andrey L. (1989). Malogabaritnyi kremnievyi akselerometr s termokompensirovannym vykhodnym signalom v diapazone temperatur ot 0 do +150°C [Small-size silicon accelerometer with temperature-compensated output signal in the temperature range from 0 to +150°C]. {X} *Vsesoyuznaya Konferentsiya. Metody i Sredstva Tenzometrii i Ikh Primenenie v Narodnom Khozyaistve*.
↩ ↩
16. Tikhomirov, M. Y., Spalek, Y. M., Borshchev, V. N., & Ponomaronko, V. v. (1989). *Method of determining resonatnt frequency of elasti element of semiconductor integral converter. Patent SU, no.* SU1516799A1 (Patent No. SU1516799A1).
↩

17. Tikhomirov, M. Yu., Osipov, V. A., Spalek Yuij M., Kharenko Konstantin Yu., & Borschev, V. N. (1986). *Method of batch production of semiconductor strain transducer elements. Patent SU, no. SU1259104A1* (Patent No. SU1259104A1). Espacenet. https://patentdb.ru/patent/1259104
↩
18. Tikhomirov, M. Y., Spalek, Y. M., & Borshchev, V. N. (1988). Temperature Dependence of Sensitivity of Silicon Integrated Mechanical Transducer in The Temperature Range from -60°C to +200°C. *Technology. Technology of Instrument Making: CSTI "Poisk"* , *13*(2 In Russian), 80–100. https://doi.org/10.13140/RG.2.2.35275.67362/1
↩ ↩ ↩
19. Galkina, E. V., & Kargin, K. A. (1988). Vliyanie temperaturnogo vozdeistviya na strukturu i fazovyi sostav.rezistivnykh plenok RS1004 [Influence of temperature exposure on the structure and phase composition of RS1004 resistive films]. *Tekhnologiya. Tekhnologiya Priborostroeniya: Nauchno-Tekhnicheskii Sbornik*, *13*(In Russian).
↩
20. Tikhomirov, M. Y., Pivonenkov, B. I., Malkov, Y. V. (1985). Kremnievyi miniatyurnyi nizkochastotnyi akselerometr [Silicon Miniature Low Frequency Accelerometer]. *Ehlektronika i Schetno-Reshayushchaya Tekhnika v Lesnoi i Derevoobrabatyvayushchei Promyshlennosti: Sbornik Nauchnykh Trudov MLTI.*, *169*(In Russian), 83–85.
↩
21. Levshina, E. S., & Novitsky, P. v. (1983). *Ehlektricheskie izmereniya fizicheskikh velichin: (Izmeritel'nye preobrazovateli) [Electrical measurements of physical quantities: (Measuring transducers)]: Vol. (In Russian).* Energoatomizdat.
↩
22. Rekleitis G., Reivindran A., Rehgsdel K. (1986). Optimizatsiya v tekhnike. [Optimization in Engineering]. (*In Russian*). http://libarch.nmu.org.ua/handle/GenofondUA/32147
↩
23. Tikhomirov, M. Y., Spalek, Y. M., Kharenko, K. Y., Giletsky, N. P., Bogatov, P. N., Yazovtsev, V. I., & Borshchev, V. N. (1977). Integrated Strain-Sensitive Element of Mechanical Transducer with Low Temperature Instability. *Technology. Technology of Instrument Making: Collection of Scientific-Technical Documents /TsNTI "Poisk"* , *3*(14), 19–27. https://doi.org/10.5281/ZENODO.7261945
↩
24. Ehleksion, M. (1986). Vnedrenie tekhnologii integral'nykh skhem v proizvodstvo datchikov [Introduction of integrated circuit technology in sensor production]. *Ehlektronika*, *11*(59 In Russian), 49–56.
↩
25. Tikhomirov, M. Y., Spalek, Y. M., Kharenko, K. Y., et al. (1988). Issledovanie, razrabotka perspektivnykh konstruktorsko-tekhnologicheskikh reshenii, obespechivayushchikh uluchshenie metrologicheskikh ehkspluatatsionnykh kharakteristik datchikov apparatury [Research and development of promising design and technological solutions that improve the metrological and operational characteristics of instrumentation sensors]. *Otchet NIR (Zakl.) [R and D Report (Final)]*, *92522.393-89*(In Russian).
↩